THE PREDICTABILITY OF NORTHERN HEMISPHERIC BLOCKING USING AN ENSEMBLE MEAN FORECAST SYSTEM

A Thesis Presented to the Faculty of the Graduate School at the University of Missouri

In Partial Fulfillment of the Requirements for the Degree

Master of Science

by

DEVONDRIA D REYNOLDS

Dr. Anthony Lupo, Thesis Advisor

MAY 2017

The undersigned, appointed by the dean of the Graduate School, have examined the thesis entitled

THE PREDICTABILITY OF NORTHERN HEMISPHERIC BLOCKING USING AN ENSEMBLE MEAN FORECAST SYSTEM

presented by DeVondria D Reynolds,

a candidate for the degree of Master of Science,

and hereby certify that, in their opinion, it is worthy of acceptance.

_____

Professor Anthony Lupo

_____

Professor Patrick Market

_____

Assistant Professor Andrew Jensen

_____

Professor Charles Nilon

ACKNOWLEDGEMENTS

Many thanks to my advisor Dr. Anthony Lupo for always believing and trusting in my work. His encouraging words and support always kept my spirits up and motivated me to succeed. I would also like to thank Dr. Market and Assistant Professor Andrew Jensen for all of their critiques and help with putting this work all together. All suggestions from all committee members are greatly appreciated and greatly improved my education and quality of this thesis. Lastly, I would like to thank God, my family and my friends for being my biggest supporters.

TABLE OF CONTENTS

LIST OF FIGURES

LIST OF TABLES

ABSTRACT

Some weather extremes can be the result of atmospheric blocking. Like atmospheric patterns that tend to repeat themselves, atmospheric blocking leads to the stagnation of weather patterns. This repetition can last for several days to weeks. These large-scale quasi-stationary mid-latitude flow regimes can result in significant temperature and precipitation anomalies in the regions that the blocking event impacts. Being able to predict periods of anomalous weather conditions due to atmospheric blocking is a major problem for medium-range forecasting. Analyzing the NCEP Ensemble 500-mb pressure heights (240 hrs.) ten-day forecasts and using the University of Missouri blocking archive to identify blocking event, the duration of blocks, intensity prediction in comparison to observed blocks. Comparing these differences over a one-year period across the Northern Hemisphere has shown the possibility for improved predictability of these blocks and their intensity. Having a better understanding of knowing how long each block will last and their associated anomalies can help society prepare for the damage they can cause. Knowing how to correctly identify blocks is important in improving forecast issues. Lastly, it is demonstrated that the Integrated Regional Enstrophy (IRE) for these events correlates with a block intensity index (BI).

CHAPTER 1: INTRODUCTION

Previous work describes or defines atmospheric blocking in a number of different ways, including as a persistent height anomaly (e.g., Shukla and Mo, 1983) or a weakness in the 500-hPa winds (e.g. Lejenas and Okland, 1983). Lupo and Smith (1995) set forth a criterion that encompasses many blocking characteristics. Here we define it as a non-linear large-scale phenomenon that occurs in the atmospheric pressure field that results in a quasi-stationary steady state in the mid-latitude flow. Cyclonic wave breaking, which results in the upscale cascade of enstrophy, is important in the maintenance of mid-latitude weather and climate (e.g. Matsueda, 2011). This cyclonic wave breaking can contribute to a persistent blocking episode, which leads to above or below average temperature and precipitation anomalies over the surrounding area caused by stagnant weather patterns (e.g. Matsueda 2011).

Matsueda (2011), Lupo et al. (2012) and many other studies examined the massive summer heat wave of 2010 in Russia resulting in more than 50,000 deaths including more then 1,600 of those resulting in drowning as people entered water to escape the heat. This heat wave caused massive economic loss, as crops were damaged. An increase in wild fires and smog levels in major Russian cities led to severe illness as well. The heat wave was the result of three atmospheric blocking events that covered the Euro-Russian region lasting from late June to early August (Lupo et al. 2012). The low

predictability of the models caused the under forecasting for extreme surface temperatures, and the decay and maintenance of the blocking events (Matsueda 2011).

Forecasters rely on numerical models to make predictions; these models are reliable out to seven days or so but limited to 10-14 days at a maximum (e.g. Lorenz 1963, 1965). Model predictions are subject to fail for various reasons, several being: parameterization errors, lack of data, measurement errors and errors in initial conditions (e.g. Lupo et al. 2016 and references therein).

1.1 Previous Work

Tibaldi et al. (1995) investigated the frequency, seasonal variability and predictability of blocking using only one model, the European Centre for Medium-Range Weather Forecasts (ECMWF). They analyzed a seven-year data set and expanding from previous work they decided to analyze for both the Northern and Southern Hemisphere year-round. The study found Atlantic blocking events to occur more in the spring while Pacific blocks were frequent in the winter with a weak peak in summer. The best blocking intensities were estimated in the spring and was over-estimated in autumn. Blocking onset was less predictable in the winter and summer in comparison to spring but the most success was predicting longevity of the blocking event. Persistent Atlantic blocks were better to predict compared to persistent Pacific blocking events. These researchers suggest that smaller case studies would be needed to figure model failures.

Colucci and Baumhefner (1997) performed a similar study to Tibaldi et al. (1995) on a 1985 winter European/Eastern Atlantic Ocean blocking event focusing on the predictability of blocking onset and the planetary/synoptic-scale conditions prior to blocking onset using forecast ensembles. They used an ensemble suite available through the Community Climate Model (CCM) of the National Center for Atmospheric Research (NCAR), which consisted of ten members. Initial data and model error were still unclear determining factors in model accuracy. Understanding that planetary scale features are predictable even when blocking isn't influenced this study. Relaxing the Colucci and Alberta (1996) criterion for blocking and setting different time leads, Colucci and Baumhefner found that more lead-time prior to blocking onset the least predictable ensemble members were and that all members failed to located the block accurately due to model systematic errors.

They concluded that neither planetary nor synoptic initial conditions were linked to uncertainty more then the model bias or model systematic errors. This suggests that even if systematic errors were identified it doesn't mean it will eliminate the model bias.

Watson and Colucci (2002) found a way to eliminate model bias by calibrating the Global Spectral Model (GSM) of the National Centers for Environmental Prediction (NCEP) ensemble forecast. Using the Brankovic et al. (1990) idea of forecasting from different times for the same day, probabilistic forecasting was created. Skill scores were calculated and tested for accuracy to create the calibrated forecast: bias, Heidke skill score (HSS) and false alarm rate (FAR) (see Wilks (1995) for more details). The

probabilistic calibrated forecast was compared to NCEP reanalysis and un-calibrated ensemble forecast and did not examine blocking maintenance or intensity. They only focused on blocking onset and frequencies during cool season from September-May 1959-1998 in both the Atlantic and Pacific region.

Watson and Colucci (2002) concluded that probabilistic calibrated forecast compared to un-calibrated ensemble forecast showed great improvements and close in accuracy to reanalysis data over the Atlantic region. Due to lack of data in the Pacific region the calibrated forecast wasn't as successful. This study proved one way to over come initial conditions uncertainty.

Lupo et al. (2016) investigated the presence of Sensitive Dependence on Initial Conditions (SDOIC) vs. Rough Dependence on Initial Conditions (RDOIC) in atmospheric phenomena and if a relationship could be developed to diagnose RDOIC as a function of observable atmospheric quantities. If the growth period of an atmospheric disturbance is longer than its characteristic time scale (based on the Reynolds number), then SDOIC will characterize the forecast of the system. This type of forecast behavior is represented by contours (e.g. a spaghetti plot) or system trajectories will diverge slowly with time. If the growth period is less than the characteristic time scale, contours will diverge exponentially with time implying predictability is not possible. In this case RDOIC would characterize the forecast of the system (Lupo et al. 2016).

One of the phenomena tested in their study was a persistent winter Pacific Region blocking event that occurred in Jan- Feb 2014. This was a noteworthy event for its

longevity and persistence; and it survived a large-scale flow regime change. Previous research has suggested that block events shouldn't survive a large-scale flow transition but the Jensen (2015) research showed that this blocking event did survive a transition. Lupo et al. (2016) found that the time scale for growth of this system was not smaller than that implied by the Reynolds number meaning this system was likely governed by quasi-geostrophic and SDOIC dynamics. The predictability of this type of event is possible in a weather forecast model.

The National Meteorological Center (NMC) started operational ensemble forecasting December 7 1992 (Toth and Kalnay 1993). Ensemble models performance has improved simulating blocking events (Matsueda 2010); this replacement from the medium-range forecast (MRF) reflects the recognition that the atmosphere is a chaotic system pointed out by Lorenz (1963).

1.2 Objectives

As opposed to previous studies that view climatological data sets with numerous blocks, this study will be similar to Lupo et al. (2016) and analyze a one year data set, focusing exclusively on four randomly chosen blocking events that occurred during that time frame. Using National Centers for Environmental Prediction (NCEP) ensemble mean forecast and NCEP/NCAR Reanalysis, a comparison will be made between model and observed climatological data for the four blocks mentioned above. The study will focus on how well the model preformed predicting blocking onset/decay, longevity,

intensity and location. Lupo et al. (2016) suggested that these atmospheric phenomena could be predicted. We suspect models will underestimate blocking intensity and decay while over-estimating or accurately predicting longevity and location. Section 2 will discuss the data and methods used to preform this research; section 3 will explain the synopses of each blocking event; section 4 will be an ensemble comparison between model and observed data and section 5 will be a conclusion and discussion of the results we found.

CHAPTER 2. DATA AND METHODOLOGY

2.1 Data Sources

Previous work has proven that ensemble forecasts preform well in predictability of high impact weather and the potential occurrence of it. Simulating blocking has greatly improved with the use of medium-range numerical weather prediction (NWP) models (Matsueda 2011). Instead of having one model solution a range of possible solutions are given. When designing the ensemble model a "probabilistic" approach was taken to use a lower-resolution (T62, equivalent to ~210km) variation of the medium-range forecast (MRF) model (Tracton and Kalnay 1993).

The National Meteorological Center (NMC), now known as the National Centers for Environmental Prediction (NCEP), developed their own ensemble forecast that once had 14 members, and now has 17 global forecast that have nearly identical initial conditions. This ensemble forecast provides several different plots that can be used for medium range forecasting. One of those is important for this research, known as the "spaghetti" plot. These ensembles mean plots consist of a single representative contour of 500-hPa heights for each member of the ensemble, which are useful in assessing the ensemble mean (Toth and Kalnay 1993).

Datasets used for this study is the NCEP Ensemble mean forecast, NCAR Reanalysis page and four Northern Hemisphere blocking events from 2016-2017. From the ensemble forecast models this study used the Northern Hemisphere 500- hPa height spaghetti plots to identify the predicted atmospheric blocking events. These 500-hPa heights were analyzed ten days out (240 hrs.) focusing on their location, duration and intensity in comparison to observed atmospheric blocking events data from the reanalysis page.

The NCEP/NCAR (National Center for Atmospheric Research) Reanalysis 1 project is used to represent observed data; there are seven sections to the Reanalysis Datasets at the PSD (National Oceanic and Atmospheric Administration's [NOAA] Earth System Research Laboratory [Physical Sciences Division]): Pressure level, surface, surface fluxes, other fluxes, tropopause, derived data and spectral coefficients. NCEP/NCAR Reanalysis 1 started in 1948 and was NOAA's first project that is an analysis/forecast system that performs data assimilations using data from 1948 to the present. NCEP used the same climate model that was initialized with a wide variety of weather observations. Some observations include ships, planes, station data, RAOBS (Radiosonde database), and GOES satellite observations just to name a few. Using this one model eliminated the complications that models changes can cause when examining climate/weather statistics and dynamic processes (Kalnay et al. 1996).

The data for this research will come from the pressure level section of the reanalysis page, Table 2.1 explains the specifications of the pressure level section and all

observed data for this research is provided by NCEP Reanalysis data products from PSD and can be found at their website: http://www.esrl.noaa.gov/psd/.

After analyzing model data information from the NCEP Ensemble models, the predicted blocking events are compared to the reanalysis system as it is used to represent the observed blocking event. These maps and all model data for this research is provided by NCEP and can be accessed through their website: https://www.esrl.noaa.gov/psd/map/images/ens/ens.html.

Table 2.1. Information from the Reanalysis project 1; specification for this research to download plots from the pressure section.

NCEP/NCAR Reanalysis 1: Pressure level section			
Temporal Coverage	Spatial Coverage	Levels	Update Schedule
• 4-times daily, daily and monthly values for 01/01/1948 to present • Long term monthly means, derived from data for years 1981-2010 • Values are instantaneous at the time indicated in the files	• 2.5 degree x 2.5 degree global grids (144 x73) • 0.0E to 357.5E, 90.0N to 90.0S	• 17 pressure levels (mb): 1000, 925, 850, 700, 600, *500, 400, 300, 250, 200, 150, 100, 70, 50, 30, 20, 10 • Some variable have less: omega (to 100mb) and humidities (to 300mb)	• Daily • 12z

During this research domain, 2016-2017 the climate presented strong and persistent blocks over the Atlantic with very few Pacific blocking events. Blocking events were selected to show diversity in how well (poorly) models behaved with blocking events that occurred in different northern hemispheric locations and different intensities. Table 2.2 describes the blocks that are going to be discussed in this research

and known as Block # here after; Block 1 is a weak and short-lived Pacific event, Block 2 is a moderate and long Atlantic event, Block 3 strong/moderate and long Pacific event, and Block 4 is a weak and short Atlantic blocking event.

Table 2.2. Description of blocking events discussed. Name, date of event/ longevity and blocking intensities from observed data. Intensities calculated are mean values over the duration of the blocking event daily.

#	Location	Date/longevity	Observed Intensity
1	Pacific (160E: 50N)	08/27/16 - 09/04/16 (8 days)	2.10
2	Atlantic (0: 55N)	10/03/16 - 10/27/16 (24 days)	3.94
3	Pacific (160W: 50N)	02/23/17 - 03/16/17 (22 days)	4.51
4	Atlantic (30E: 50N)	06/24/16 - 07/08/16 (14 days)	2.46

2.2 Methods

In order to identify observed and model blocking events the criteria for blocking used in this study is the Lupo and Smith (1995) criteria which is the following conditions from their publication:

1. The Rex (1950) criteria must be satisfied for an anticylonic flow region at 500 hPa with the exception that the minimum duration must be 5 days (Triedl et al. 1981).
2. A negative or small positive Lejenas and Okland (1983) index must be present on a Hovmöler diagram in the Northern Hemisphere.
3. Conditions 1 and 2 must be satisfied together from 24 hour after onset to 24 hour before termination.

4. The anticyclone should be poleward of 35° N or 35° S and the ridge should have an amplitude of greater than 5 °latitude.
5. Block onset is described to occur when condition 4 and or conditions 1 or 2 are met.
6. Termination is designated at the time the event fails condition 5 for a 24-hour period or longer (Wiedenmann et al. 2002).

Please see Lejenas and Okland (1983) and Lupo et al. (1997) more information. This criterion was used to determine the four blocks discussed in this study.

The purpose of this study is to show the quality of the model's performance, in comparison to observed events, in reference to the predictability of the blocking events longevity, onset and termination and intensity. In order to determine blocks intensity Lupo and Smith (1995) introduced a quantity known as blocking intensity index (BI) and Wiedenmann et al. (2002) modified BI for automated use and is defined as equation 2.1:

$$BI = \frac{\frac{Center}{\left(\frac{lowest\ upstream+center}{2}\right)+\left(\frac{lowest\ downstream+center}{2}\right)}}{2} \qquad (2.1)$$

The intensity for blocking is proportional to the strength of mid-latitude height gradients. Figure 2.1 explains how you can find the values for the blocking intensity equation.

Looking at a 500-hPa height plot, when an atmospheric blocking event occurs it has a blocking center that is present on some degree of latitude. The height value at the blocking center is the numerator value. To find the lowest upstream and downstream value, start from the center height follow the same degree of latitude (upstream or downstream) to the next trof axis. At that point you can determine the height value and put those values into the equation to determine BI.

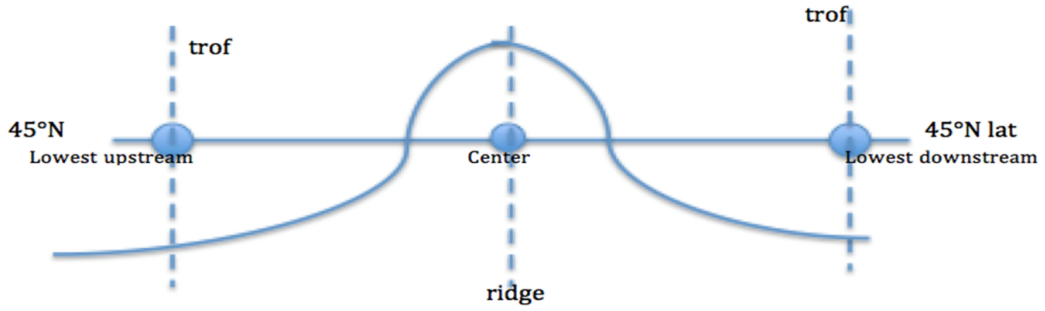

Figure 2.1. Diagram created to explain how to determine values for BI equation.

To determine the preformance of the ensemble mean model the amount of lead time the models predict a block to be present will determine the quality of the forecast projected. This study will also discuss possibilities to improving forecast by the use of enstophy and its integral, Intergrated Regional Enstrophy (IRE) has been proven to be useful dianositics in identifying blocking-regime transition (Jensen and Lupo 2013). This technique uses local Lyapunov exponents for the bartropic voriticy equation.

Dymnikov et al. (1992) describes blocking as a quasi-stationary atmospheric state with quasi-barotropic structure, in a quasi-barotropic flow the sum of the positive

Lyapunov exponents is related to IRE. Lyapunov exponents is the measure of the divergence or convergence of system trajectories that are close and can be approximated by integrating enstrophy over a finite region known as IRE, which is squared vorticty (Lupo and Jensen 2016). Lupo et al., (2007) used this technique to determine the stability or predictability within a planetry flow regieme.

Some of these techniques will be used in this study to assist in increasing predictability of atmospheric blocking. Integrate Regional Enstrophy (IRE) is calculated following Lupo et al. (2012). Here IRE is defined as:

$$Enstrophy = \sum_{\lambda_i>0} \lambda_i \approx \int \zeta^2 \tag{2.2}$$

This value can be used as a mesure of predictability, higher values correspond to a lesser degree of predictabilty or possibly the transitioning of atmospheric flow, while lower values correspond to a greater degree of predictability in a more stable flow configuration (e.g. Lupo et al. 2012). To calculate this quantity the following procedures and equation were used:

$$\zeta_g = \frac{g}{f}\nabla^2 z \tag{2.3}$$

Enstophy is the square of the geostrophic relative vorticity, where the quantity z is the 500 hPa height field. Differentials were calculated using second order finite differencing over a 10° latitude by 10° longitude grid box encompassing the center of the blocking event.

CHAPTER 3: SYNOPTIC DISCUSSION

3.1 Block 1: Pacific Weak

Blocking event one was located over the Pacific Ocean and persisted for eight days. This block began August 27th 2016 and decayed on September 4th 2016. Wiedenmann et al. (2002) stratified a 30-year sample of blocking events and rated blocking intensity from strength of 1 – 10, 10 being the strongest. Table 3.1 explains the rationale rates blocking intensities as the following:

Table 3.1. Blocking Intensity index from Wiedenmann et al. (2002) describing what a BI value would represent in degree of strength.

Blocking strength	
BI	Strength
<2.0	Weak
2.0<BI<4.3	Moderate
>4.3	Strong

This block was ranked as a moderate event with an average of 2.10, which is normal for blocking events that occur during the warm season (cold season: October-April e.g. Wiedenmann et al. 2002). Wiedenmann et al. (2002) found that cold season and oceanic region blocks were stronger in their research compared to warm season or continental blocking events. Block one shifted in location during its tenure from 50°N in

latitude and stayed in the 40°N range for several days and shifting back towards 70° N as it decayed. The intensity of the block changed some as well but was similar in strength at the beginning and end. At onset the block was weak at 1.81 BI and continued to increase to 2.97 BI in the middle of its duration on August 31 2016, thereafter BI decreased to 1.60.

During the time of blocking onset and decay, the Integrated Regional Enstrophy (IRE) has shown to increase demonstrating planetary-scale instability. Based on the idea that planetary-scale flow has shown to coincide with blocking transition regime, Figures 3.1.1 and 3.1.2 show the relationship between BI and enstrophy, previous work has demonstrated that BI nearly increases linearly in proportion to the upstream and downstream height gradient (Wiedenmann et al. 2002). Taking a look at both Figure 3.1.1 and Figure 3.1.2 both enstrophy and blocking intensity start and end the same way with low onset and decay values but not for the duration of the event. There is a low negative correlation between the two, a correlation value of -0.14. Block 1 showed to be chaotic during the peak in BI.

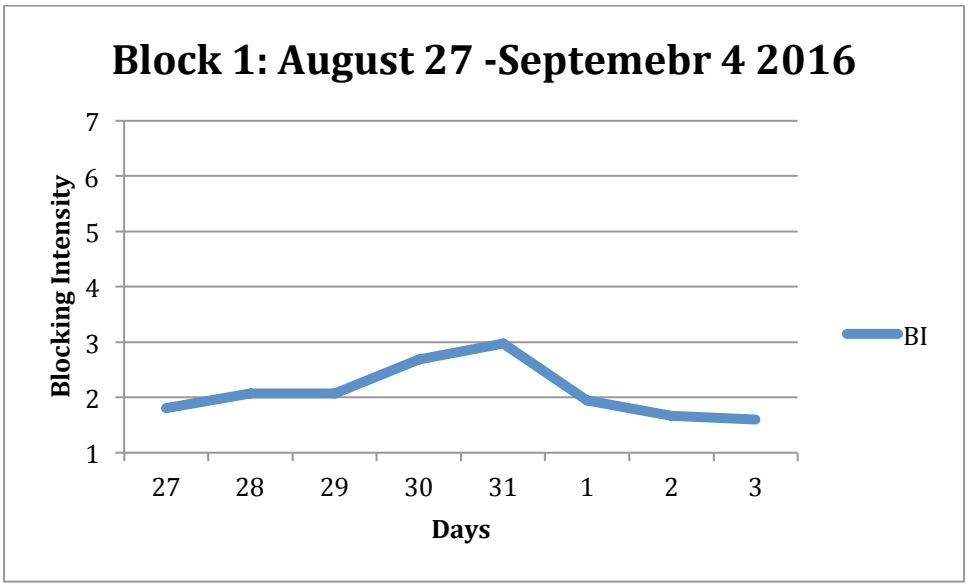

Figure 3.1.1. Graph of blocking intensity (BI) during Block 1 duration.

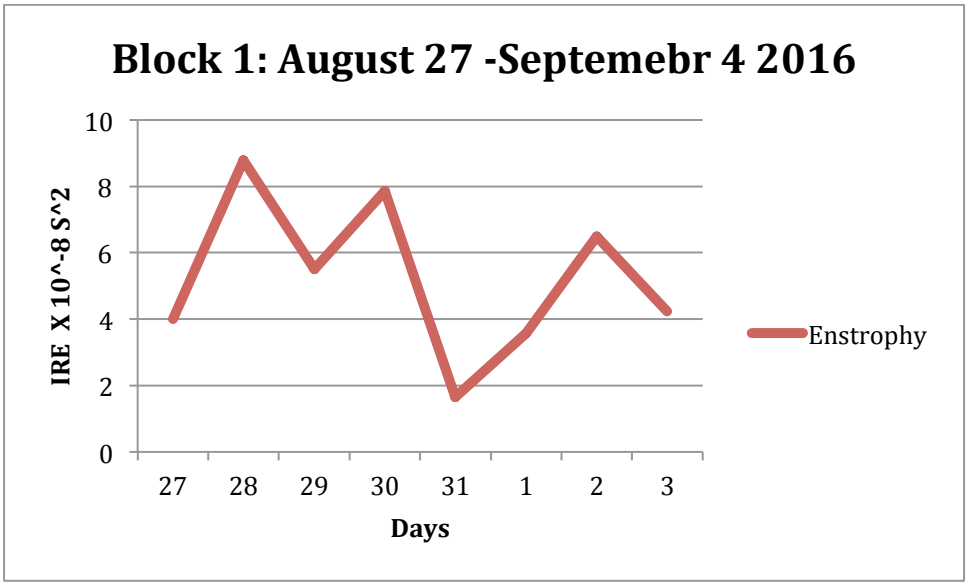

Figure 3.1.2. Graph of Enstrophy during Block 1 duration.

3.2 Block 2: Atlantic Strong

Blocking event two was located in the Atlantic Ocean and observed lasting 24 days. This block began October 3rd 2016 and decayed on October 27th 2016 with an average blocking intensity of 3.94, which is normal for a blocking event during the cold season, as these blocks tend to be stronger then warmer season events.

Block two shifted in location during its tenure from 55°N in latitude and stayed in the 60°N range for several days and shifting back towards 70° N. While in the 70° N range, BI was at maximum reaching up to 6.03, and lowering back to low moderate strengths, shifting in location back to 50°N as it decayed.

Figure 3.2.1 and Figure 3.2.2 show there is a low positive correlation between enstrophy and BI in Block 2 of 0.26. Enstrophy does show a maximum towards decay and onset suggesting flow regime transformation. Although not as strong, they both correlate in peak values as well for the duration of the event with enstrophy.

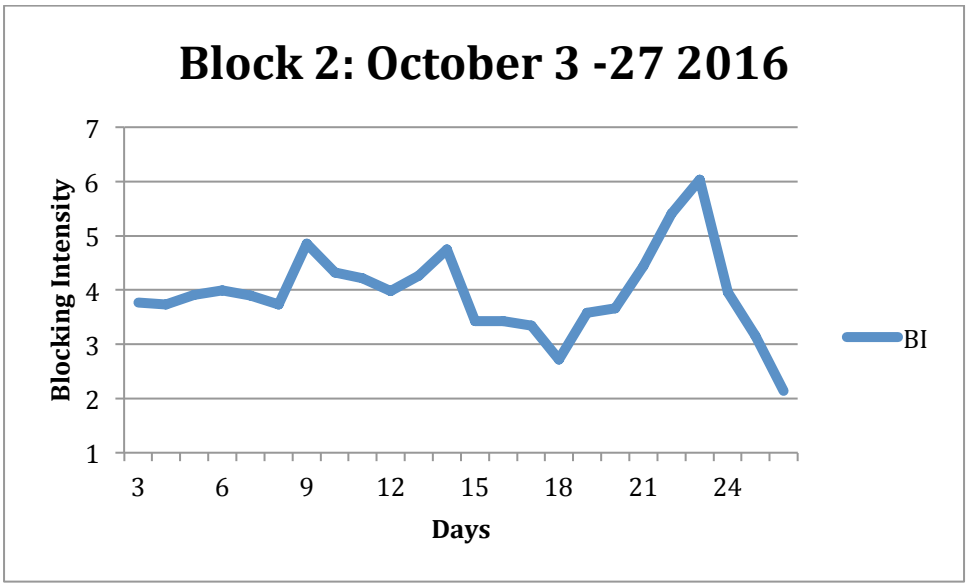

Figure 3.2.1. Graph of blocking intensity during Block 2 duration.

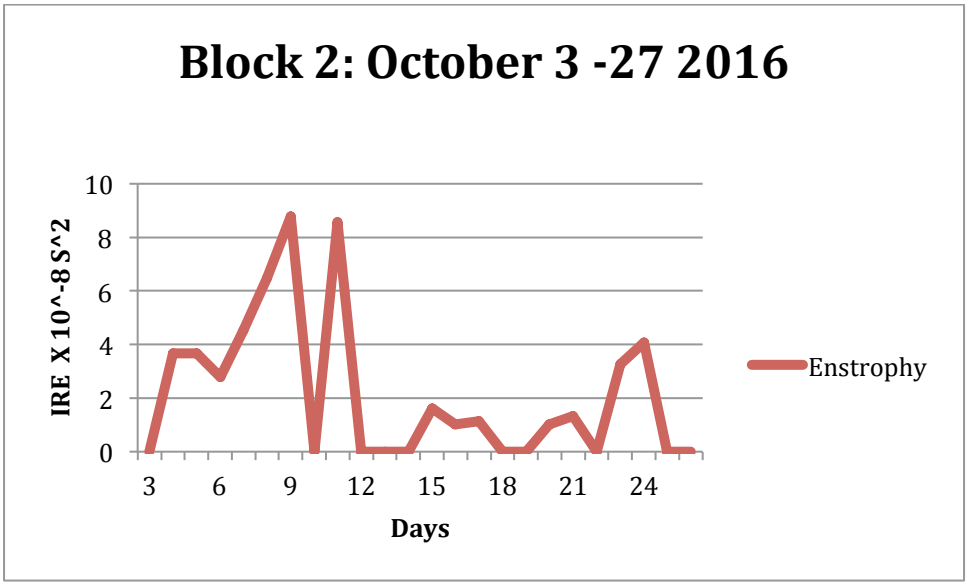

Figure 3.2.2. Graph of Enstrophy during Block 2 duration.

3.3 Block 3: Pacific Strong

Blocking event three was located over the Pacific Ocean and persisted twenty-two days, began on February 23rd and decayed March 16th 2017. The block was ranked strong which is normal, as in the cold season oceanic blocks showed to be stronger compared to warm season continental blocks with an average intensity of 4.51. Block 3 shifted slightly in location from 50° N latitude to 45° N latitude until the beginning of March, block 3 shifted from 50° N and back down to 45° N. This shift in location caused for a deeper look into this events behavior in comparison to the blocking criterion. After analyzing deeper we decided this was one massive blocking event not two. For the remaining of this blocks tenure it flirted between 55 and 50° N and remained at 55° N several days until its decay. BI reached maximum intensity of 5.69 during its location change and reached its minimum 3.24 BI at decay. During the decay IRE showed to increase, Figures 3.4.1 and 3.4.2 show the relationship between BI and enstrophy.

BI and enstrophy showed a low negative correlation of -0.10. At both onset and decay BI and enstrophy showed high negative correlation as IRE increased (decreased) BI decreased (increased). They had a relative similar trend just in opposite directions.

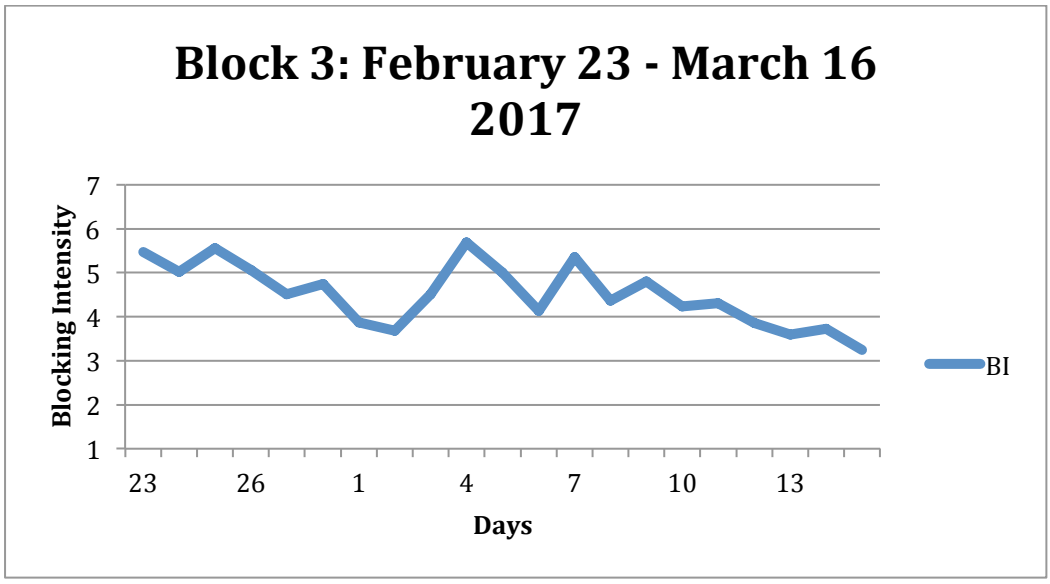

Figure 3.3.1. Graph of blocking intensity during Block 3 duration.

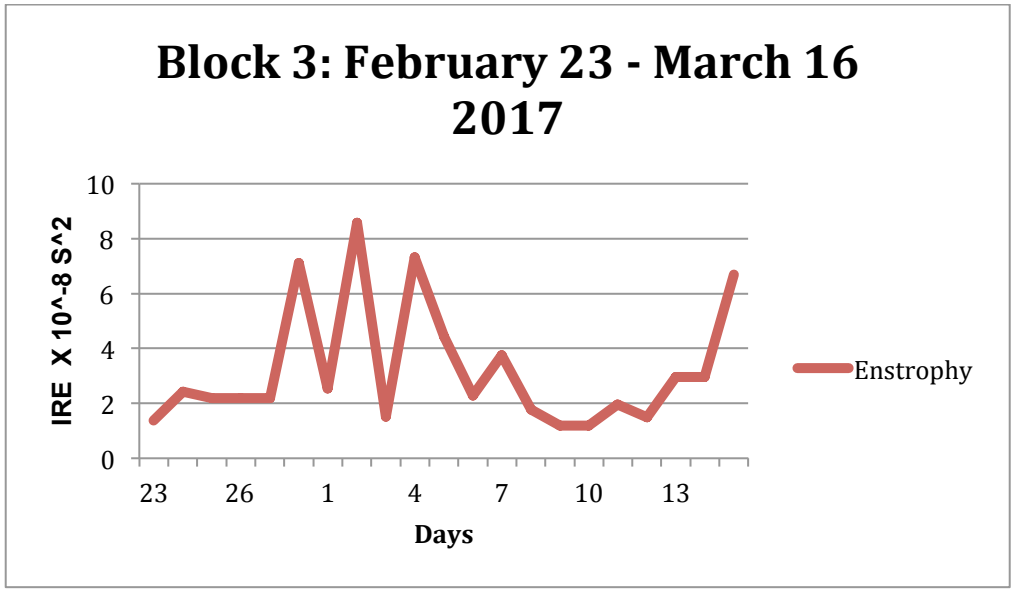

Figure 3.3.2. Graph of IRE during Block 3 duration.

3.4 Block 4: Pacific Weak

Blocking event 4 was located in the Pacific Ocean and observed lasting 14 days. The block began June 24th 2016 and decayed on July 8th 2016 with an average blocking intensity of 2.46, ranking as moderate, which is normal for block during the warm season, as these blocks tend to be weaker the cold season events.

Block 4 shifted in location during its tenure from 50°N in latitude and shifted from the 50°N latitude range to the 60°N range for several days and shifting back towards 70° N towards its demise. BI remained at moderate strength during its life cycle ranging from 2.14 – 2.82 BI.

Figure 3.4.1 and Figure 3.4.2 show there is a low positive correlation of 0.05 between enstrophy and BI in Block 4 similar to Block 2. Peak values trend and enstrophy does show a spike in high values towards decay and onset.

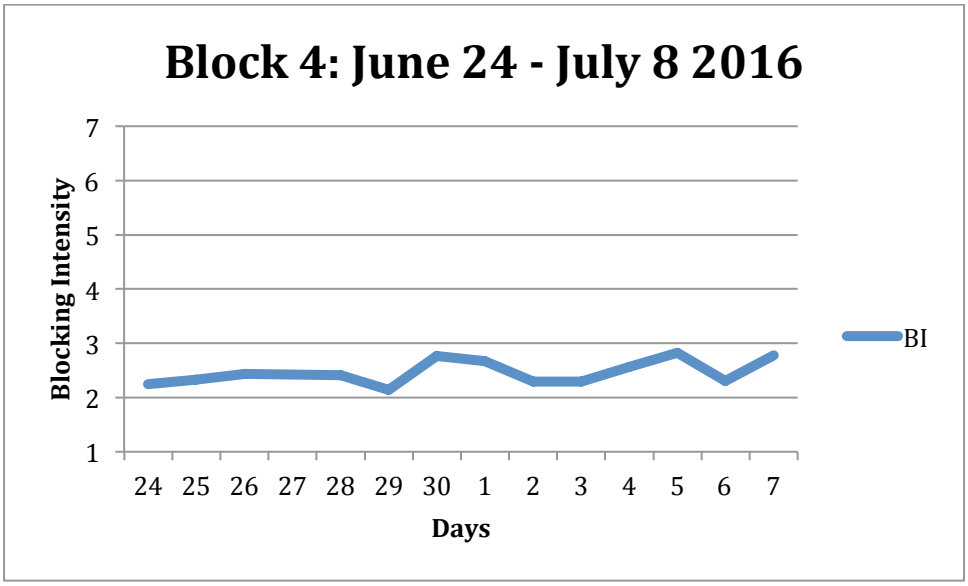

Figure 3.4.1. Graph of blocking intensity during Block 4 duration.

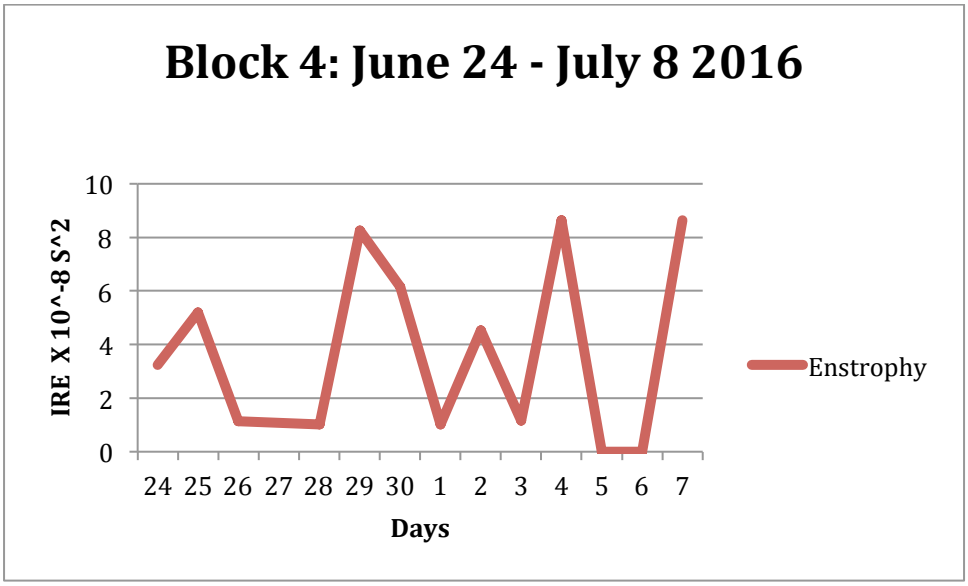

Figure 3.4.2. Graph of enstrophy during Block 4 duration.

3.5 Correlation

Lupo and Smith (1995) and Lupo (1997) showed that during block onset, deepening cyclonic disturbances would result in increased block center 500-hPa heights. Each of these events was preceded by a rapidly developing cyclone (See Fig. 3.5). Then IRE peaked following onset. The IRE peaks may be associated with peaks in the synoptic-scale component of the height field as shown in Lupo et al. (2012) for the July 2010 blocking event, which occurred over Russia. These peaks are likely associated with the deepening synoptic scale cyclone. Then it might be expected that the BI maxima may occur near the time of the IRE maxima as in Jensen (2015).

To test this proposal correlation was performed with and without enstrophy time lag up to 72 hours. Higher positive correlations were achieved for Block 1 and 4 (0.39 and 0.52, respectively) if the time series were lagged by 24 hours such that BI leads IRE. For blocking event 2, the best correlation (0.26) was achieved with no lag. Block 3 achieved the best correlation (0.47) when BI leads IRE by 72 hours. Lagging the IRE time series such that BI leads IRE produces higher correlations closer to one. Thus, we can describe block onset as in Lupo and Smith (1995), and then maxima in IRE will occur at or following block onset, followed by a maximum in BI at or following these events. Table 3.2 shows the correlations in detail and with respect to being lagged where BI leads IRE.

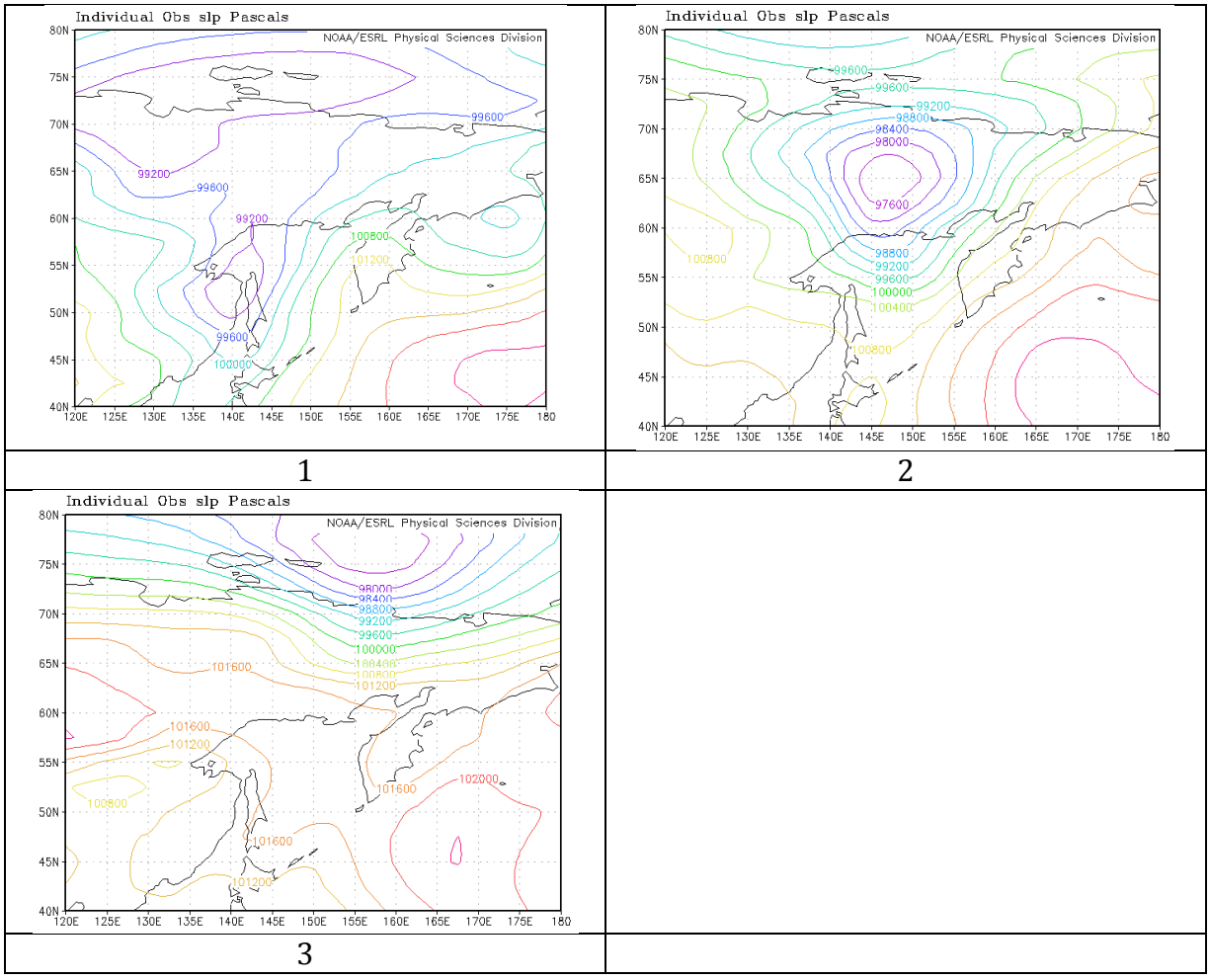

Figure 3.5. This is an example of one of the upstream cyclones. This is for Block 1 12Z 27 August 2016. 1st panel is SLP at 12Z 25 August; central pressure is about 990 hPa. 2nd is 12z 26 August central pressure about 973 hPa and 3rd is 12Z 27 August and the central pressure is about 973 hPa.

Table 3.2. How the effect of lagging IRE improves correlations between BI and IRE, PW: Pacific Weak, AS: Atlantic Strong, PS: Pacific Strong, AW: Atlantic Weak, *best correlation.

Correlation with lag				
	Not Lagged	24- Hr.	48-Hr.	72-Hr.
Block 1: PW	-0.14	.38	.57 *	.40
Block 2: AS	0.26 *	.09	.04	.10
Block 3: PS	-0.10	-0.09	.18	.47 *
Block 4: AW	.05	.52 *	-0.38	.15

CHAPTER 4: ENSEMBLE COMPARISON

To get a better understanding of how well the models preformed we investigated how many days lead-time the model predict any potential for a blocking event to occur. Focusing on seven-day, four-day, and one-day out forecast with each forecast day having a ten-day outlook. We also compared the forecast blocking intensity to the observed blocking intensity.

4.1 Block 1: August 27 – September 4 2016 Lead-time forecast

The ensemble model mean seven-day forecast for Block 1 showed no presence of a block for the entire ten-day outlook. The ensemble model four-day forecast did show a blocking event present but struggled with the onset date. There was some indication on the target date of August 27 2016 that a block would be present but the structure did not last. The four-day forecast showed a valid block from August 29 – September 1 not lasting till end of the ten-day outlook. Table 4.1 shows the comparison in blocking intensity of the ensemble model forecast vs. observed blocking event during the validation period of the four-day and one-day forecast. The ensemble models still struggled with the onset of Block 1 for the one-day forecast showing a block to be present August 29 2016 – September 1.

The ensemble models struggled with the presence of a block with longer lead times and with both the onset and decay of this block and the how intense the block would be during its forecasted period. The models didn't show any significant presence of a block until August 29 2016 for both the four-day and one-day outlook. The validation periods were the same cutting the block short of three days before its actual decay. Figure 4.1 is a comparison of Block 1 during the seven-day forecast. For this specific forecast day the models did agree that there was some form of a block was present, but not in the correct location. Using Rex (1950) criterion it was determined that the model didn't predict presence of a block.

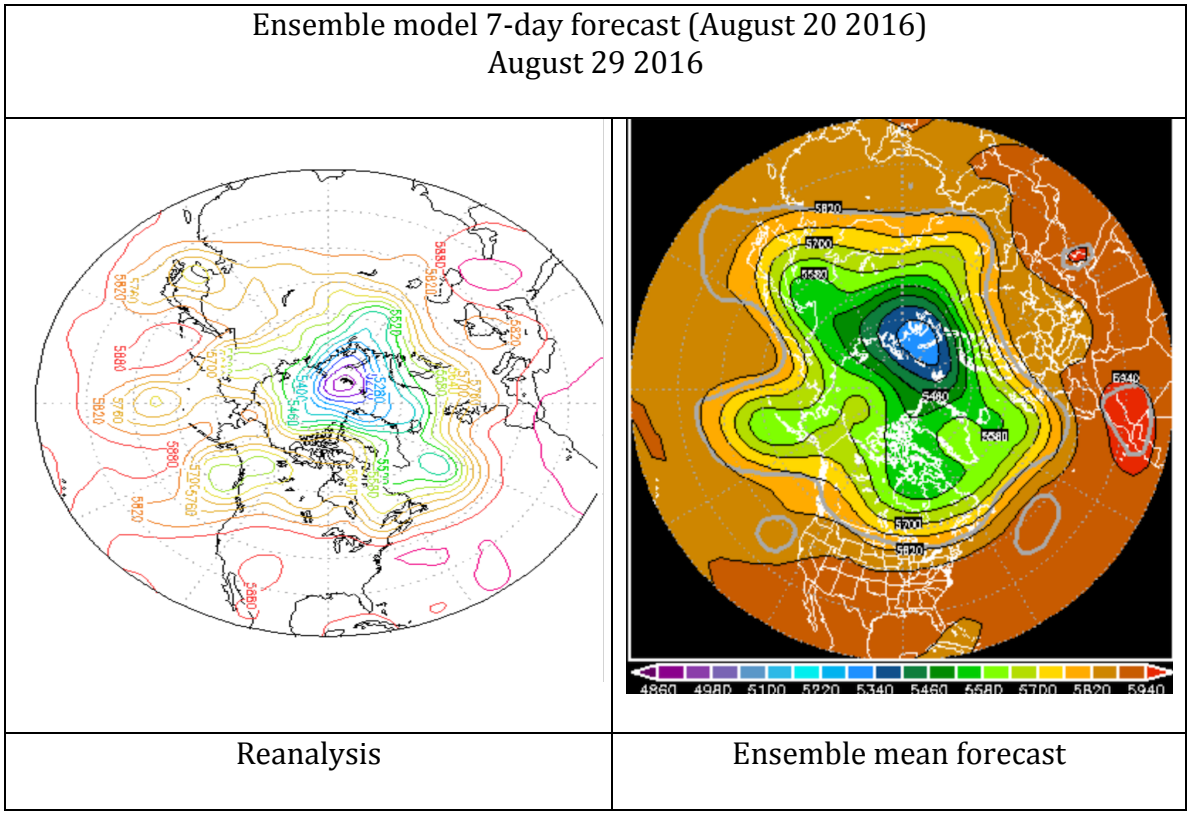

Figure 4.1. Represents a comparison of the seven-day forecast 48 hours into blocking event onset. Reanalysis (left) vs. NCEP ensemble mean 216+ hr. forecast (right).

4.2 Block 2: October 3 – October 27 2016 Lead-time forecast

Similar to Block 1, the ensemble model seven-day forecast for Block 2 showed no presence of a block for the entire ten-day outlook and the ensemble model four-day forecast struggled with onset as well. The models show a block present from October 5-October 9, considering how long and strong this block was the model significantly under preformed. Table 4.1 shows the comparison in blocking intensity of the ensemble model forecast vs. observed blocking event during the validation period of the four-day and one-day forecast.

The ensemble mean one-day forecast preformed slightly better with onset and longevity. The models showed a block present from October 4- October 11, just one day shy from the target date of October 3 and just one day shy from the complete ten day outlook knowing this event lasted far past a ten day outlook from October 2.

Similar to Block 1 the ensemble models struggled with the presence of a block with longer lead times and with both the onset and decay of this block and the how intense the block would be during its forecasted period. Although the models struggled they did represent onset better with shorter lead-times and blocking intensity wasn't as bad but still under forecasted. Figure 4.2 is a comparison of Block 2 during the four-day forecast. At this forecast time ensemble models struggled with the block intensity but handled the location well.

Ensemble model 4-day forecast (September 29 2016) October 5 2016	
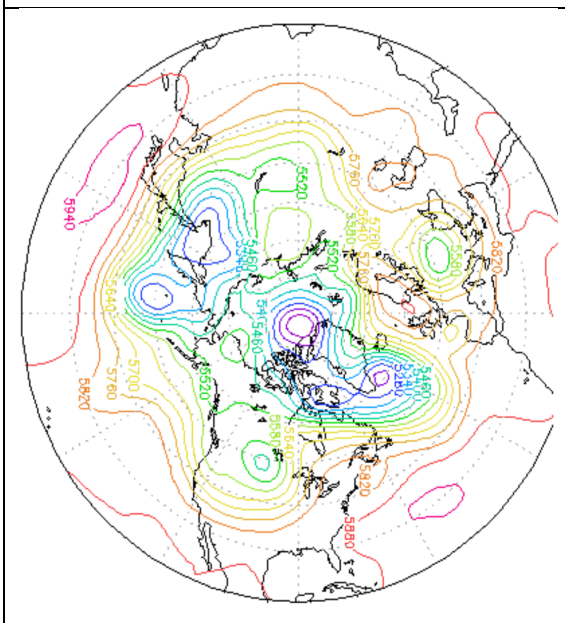	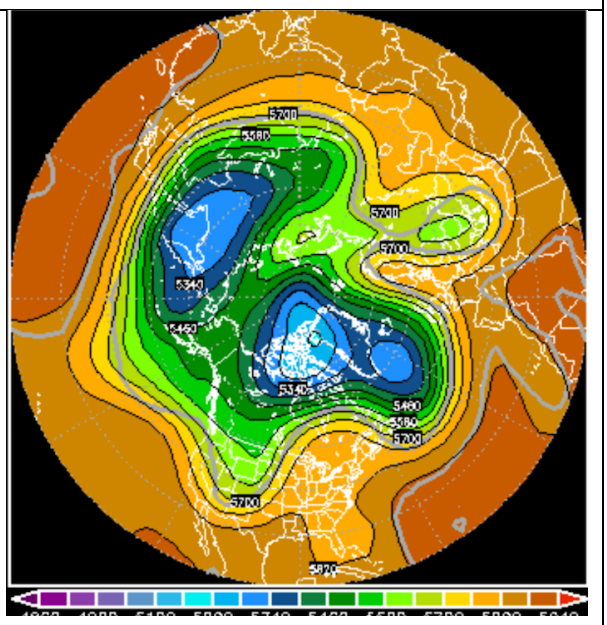
Reanalysis BI: 3.91	Ensemble mean forecast BI: 2.30

Figure 4.2. Represents a comparison of the seven-day forecast 48 hours into blocking event onset. Reanalysis (left) vs. NCEP ensemble mean 144+ hr. forecast (right).

4.3 Block 3: February 23 – March 16 2017 Lead-time forecast

Like blocks previously mentioned Block 3 did struggle with longer lead-time and block not persisting but there was at least a block present for the day seven-day forecast. Block 3 seven-day forecast showed a block present 24 hours after the onset date from February 24 – February 26. Table 4.1 shows the comparison in blocking intensity of the ensemble model forecast vs. observed blocking event during the validation period of the seven-day, four-day, one-day forecast.

As lead times decreased models handled Block 3 maintenance, onset, decay and location very well. The four-day forecast showed a block present from February 23 – February 27. Model agreement wasn't as strong to qualify blocking past the 27th but models did attempt to show the presence of a block up until March 1. The one-day forecast showed strong block presence from February 23-March 1 and over –estimated blocking onset by 24 hours. Model agreement wasn't as strong to qualify blocking past the 1st but models did attempt to show presence for the entire 10-day outlook. Figure 4.3 is a comparison of Block 3 during the seven-day forecast. Ensemble mean forecast struggled both with location and BI.

Ensemble model 7-day forecast (February 16 2017) February 25 2017	
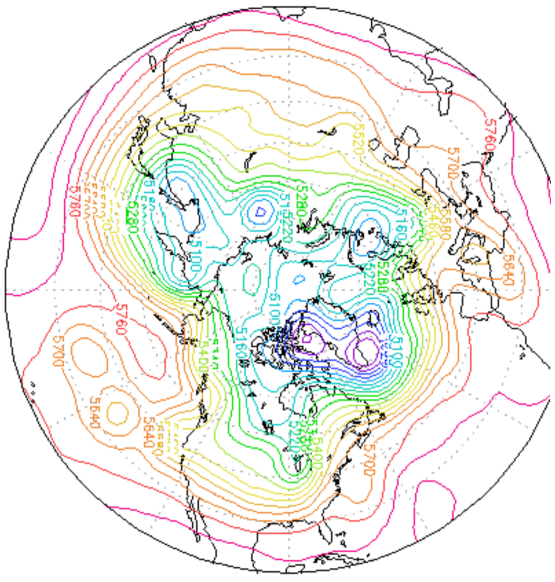	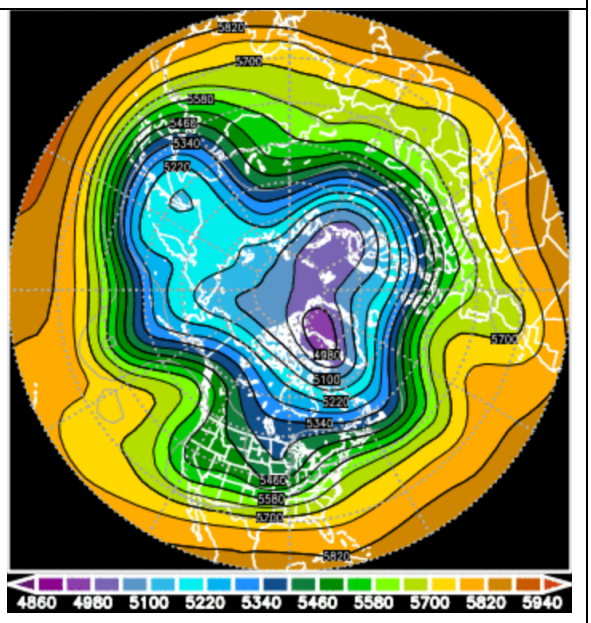
Reanalysis BI: 5.56	Ensemble mean forecast BI: 2.99

Figure 4.3. Represents a comparison of the seven-day forecast 48 hours into blocking event onset. Reanalysis (left) vs. NCEP ensemble mean 216+ hr. forecast (right).

4.4 Block 4: June 24 – July 8 2016 Lead-time forecast

As with blocks mentioned previously longer lead times showed no blocks present. Block 4 seven-day and four-day ensemble mean forecast showed no presence of a block for the entire ten-day outlook. Model performance during this blocking event was very poor until the event was actually taking place. The ensemble one-day forecast showed a block present from only June 24 – June 26. Models forecasted onset accurately but under performed in longevity. The models should have lasted through the entire ten-day outlook before decaying. Table 4.1 shows the comparison in blocking intensity of the ensemble model forecast vs. observed blocking event during the validation period of the one-day forecast. Figure 4.4 is a comparison of Block 4 during the one-day forecast. Ensemble mean forecast predicted location accurately but struggled with BI.

Ensemble model 1-day forecast (June 23 2016) June 26 2016	
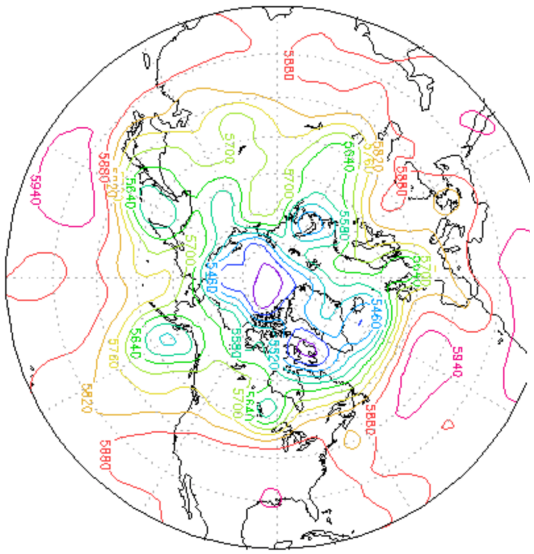	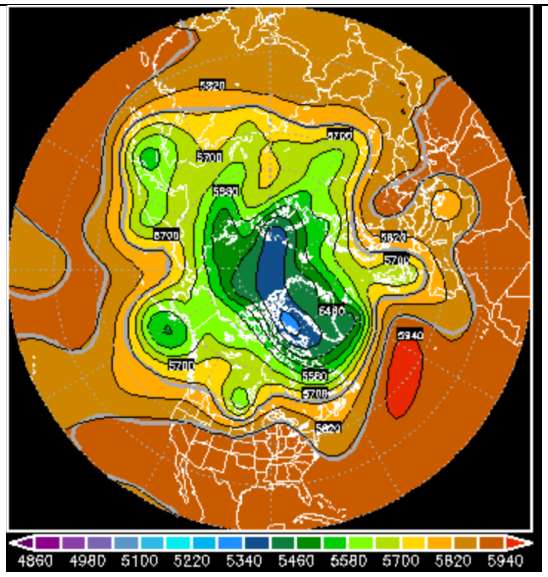
Reanalysis BI: 2.43	Ensemble mean forecast BI: 1.20

Figure 4.4. Represents a comparison of the seven-day forecast 48 hours into blocking event onset. Reanalysis (left) vs. NCEP ensemble mean 72+ hr. forecast (right).

Table 4.1. Shows the comparison in blocking intensity of the ensemble model forecast vs. observed blocking event during the validation period of all seven-day, four-day and one-day forecast for all four blocking events. N/A: no block present.

BI Comparison			
Forecast /Blocks	Model BI	Observed BI	Difference
7 day			
Block 1: AW 08/20/2016	N/A	N/A	N/A
Block 2: AS 09/26/2016	N/A	N/A	N/A
Block 3: PS 02/16/2017	2.87	5.13	2.26
Block 4: PW 06/17/2016	N/A	N/A	N/A
4 day			
Block 1: AW 08/23/2016	.39	2.42	2.03
Block 2: AS 09/29/2016	2.43	4.08	1.65
Block 3: PS 02/19/2017	3.73	4.89	1.16
Block 4: PW 06/20/2016	N/A	N/A	N/A
1 day			
Block 1: AW 08/26/2016	.93	2.27	1.34
Block 2: AS 10/02/2016	2.90	4.08	1.18
Block 3: PS 02/22/2017	2.52	5.22	2.70
Block 4: PW 06/23/2016	1.24	2.34	1.10

CHAPTER 5: CONCLUSION

Four blocking events were compared, two in the Atlantic and two and the Pacific region using the NCEP/NCAR reanalysis data focusing on the ability of an ensemble mean model forecast (NCEP) to predict blocking intensity, longevity, onset, decay and location. Here we used the 500-hPa heights and the Wiedenmann et al. (2002) criterion to identify blocking. Additionally, the IRE was calculated and compared to the BI.

Overall in all cases location, the model best captured decay and longevity while blocking intensity and onset were underestimated, blocking intensity having the worst performance. Enstrophy was introduced to determine if there could be a relationship that could be developed to diagnose IRE as a function of observable atmospheric quantities for intensity. For this study correlation wasn't as high as we could have hoped for or expected during the blocking events entire longevity. Although BI and IRE didn't correlate for the entire time period it did show a correlation during onset and decay and with the help of lag, correlations can increase. In the future, in order to expand on this work it is possible to introduce Watson and Colucci (2002) probabilistic forecast to increase accuracy in blocking intensity and onset.

Ensemble mean forecast struggled with blocking intensities especially with the strong persistent blocks. Predicting BI, Block 4 had the best one-day lead-time, Block 2 had the best four-day lead-time and Block 3 was the only block to have a seven-day lead-time to show any blocking event present. Compared to Tibaldi et al. (1994) results, Blocks 2 and 3 showed to be exact opposite of their findings. Instead of the Pacific

blocking event being difficult to predict it was the Atlantic block that showed difficulty in location, longevity and blocking intensity.

REFERENCES

A.D. Jensen and A.R. Lupo, "Using Enstrophy as a Diagnostic to Identify Blocking Regime Transi- tion," Q.J.R. Meteorol. Soc., DOI: 10.1002/qj.2248, 2013.

Andrew D. Jensen, "A Dynamic Analysis of a Record Breaking Winter Season Blocking Event," Advances in Meteorology, vol. 2015, Article ID 634896, 9 pages, 2015. doi:10.1155/2015/634896

Anthony R. Lupo, Igor I. Mokhov, Yury G. Chendev, Maria G. Lebedeva, Mirseid Akperov, and Jason A. Hubbart, "Studying Summer Season Drought in Western Russia," Advances in Meteorology, vol. 2014, Article ID 942027, 9 pages, 2014. doi:10.1155/2014/942027

Brankovic, C., T. N. Palmer, F. Molteni, S. Tibaldi, and U. Cubasch, 1990: Extended-range predictions with ECMWF models: Time-lagged ensemble forecasting. *Quart. J. Roy. Meteor Soc.*, **116,** 857–912.

Colucci, S.J. and T.L. Alberta, 1996: Planetary-Scale Climatology of Explosive Cyclogenesis and Blocking. *Mon. Wea. Rev.,* **124**, 2509–2520, doi: 10.1175/1520-0493(1996)124<2509:PSCOEC>2.0.CO;2.

Colucci, S.J. and D.P. Baumhefner, 1998: Numerical Prediction of the Onset of Blocking: A Case Study with Forecast Ensembles. *Mon. Wea. Rev.,* **126**, 773–784, doi: 10.1175/1520-0493(1998)126<0773:NPOTOO>2.0.CO;2.

Dymnikov VP, Kazantsev YV, Kharin VV. 1992. Information entropy and local Lyapunov exponents of barotropic atmospheric circulation. *Izv. Atmos. Oceanic Phys.* **28**: 425–432.

Kalnay, E.E., M.M. Kanamitsu, R.R. Kistler, W.W. Collins, D.D. Deaven, L.L. Gandin, M.M. Iredell, S.S. Saha, G.G. White, J.J. Woollen, Y.Y. Zhu, A.A. Leetmaa, R.R. Reynolds, M.M. Chelliah, W.W. Ebisuzaki, W.W. Higgins, J.J. Janowiak, C.C. Ropelewski, J.J. Wang, R. Jenne, and D. Joseph, 1996: The NCEP/NCAR 40-Year Reanalysis Project. *Bull. Amer. Meteor. Soc.,* **77**, 437–471, doi: 10.1175/1520-0477(1996)077<0437:TNYRP>2.0.CO;2.

Lejenas, H., 1984: Characteristics of Southern Hemisphere blocking as determined from a time series of observational data. *Quart. J. Roy. Meteor. Soc.*, **110,** 967–979.

Lejenas, H., and H. Okland, 1983: Characteristics of Northern Hemisphere blocking as determined from a long time series of observational

data. *Tellus*, **35A,** 350–362.

Lorenz, E.N., 1963: Deterministic Nonperiodic Flow. *J. Atmos. Sci.,* **20**, 130–141, doi: 10.1175/1520-0469(1963)020<0130:DNF>2.0.CO;2.

Lupo, A., Y. Li, Z. Feng, N. Fox, J. Rabinowitz, and M. Simpson, 2016: Sensitive versus Rough Dependence under Initial Conditions in Atmospheric Flow Regimes. *Atmosphere*, **7**, 157, doi:10.3390/atmos7120157. http://dx.doi.org/10.3390/atmos7120157.

Lupo, A.; Jensen, A. Integrated Regional Enstropy as a Measure of Kolmogorov Entropy. *In Proceedings of the 1st Int. Electron. Conf. Atmos. Sci.*, 16–31 July 2016; Sciforum Electronic Conference Series, Vol. 1, 2016 , C003; doi:10.3390/ecas2016-C003

Lupo, A.R., 1997: A Diagnosis of Two Blocking Events That Occurred Simultaneously in the Midlatitude Northern Hemisphere. *Mon. Wea. Rev.,* **125**, 1801–1823, doi: 10.1175/1520-0493(1997)125<1801:ADOTBE>2.0.CO;2.

Lupo, A. R., and P. J. Smith, 1995a: Climatological features of blocking anticyclones in the Northern Hemisphere. *Tellus*, **47A,** 439–456.

Lupo AR, Mokhov II, Dostoglou S, Kunz AR, Burkhardt JP. 2007. The impact of the planetary scale on the decay of blocking and the use of phase diagrams and enstrophy as a diagnostic. *Izv. Atmos. Oceanic Phys.* **42**: 45–51.

Lupo AR, Mokhov II, Akperov MG, Cherokulsky AV, Athar H. 2012. A dynamic analysis of the role of the planetary and synoptic scale in the summer of 2010 blocking episodes over the European part of Russia. *Adv. Meteorol.* **2012**: Article ID 584257; 11pp, Doi: 10.1155/2012/584257.

Matsueda, M., M. Kyouda, Z. Toth, H.L. Tanaka, and T. Tsuyuki, 2011: Predictability of an Atmospheric Blocking Event that Occurred on 15 December 2005. *Mon. Wea. Rev.,* **139**, 2455–2470, doi: 10.1175/2010MWR3551.1.

Rex, D. F., 1950: Blocking action in the middle troposphere and its effect on regional climate II: The climatology of blocking action. *Tellus*, **3,** 275–301.

Shukla, J.J. and K.C. Mo, 1983: Seasonal and Geographical Variation of Blocking. *Mon. Wea. Rev.,* **111**, 388–402, doi: 10.1175/1520-0493(1983)111<0388:SAGVOB>2.0.CO;2.

Shutts, G. J., 1983: The propagation of eddies in diffluent jet streams: Eddy vorticity forcing of blocking flow fields. *Quart. J. Roy. Meteor. Soc.*, **109,** 737–761

Tibaldi, S.S., E.E. Tosi, A.A. Navarra, and L.L. Pedulli, 1994: Northern and Southern Hemisphere Seasonal Variability of Blocking Frequency and Predictability. *Mon. Wea. Rev.,* **122**, 1971–2003, doi: 10.1175/1520-0493(1994)122<1971:NASHSV>2.0.CO;2.

The NCEP/NCAR 40-Year Reanalysis Project: March, 1996 BAMS

Tracton, M. and E. Kalnay, 1993: Operational Ensemble Prediction at the National Meteorological Center: Practical Aspects. *Wea. Forecasting,* **8**, 379–398, doi: 10.1175/1520-0434(1993)008<0379:OEPATN>2.0.CO;2.

Triedl, R. A., E. C. Birch, and P. Sajecki, 1981: Blocking action in the Northern Hemisphere: A climatological study. *Atmos.–Ocean*, **19,** 1–23.

Toth, Z. and E. Kalnay, 1993: Ensemble Forecasting at NMC: The Generation of Perturbations. *Bull. Amer. Meteor. Soc.,* **74**, 2317–2330, doi: 10.1175/1520-0477(1993)074<2317:EFANTG>2.0.CO;2.

Tyrlis, E.E. and B.J. Hoskins, 2008: The Morphology of Northern Hemisphere Blocking. *J. Atmos. Sci.,* **65**, 1653–1665, doi: 10.1175/2007JAS2338.1.

Watson, J.S. and S.J. Colucci, 2002: Evaluation of Ensemble Predictions of Blocking in the NCEP Global Spectral Model. *Mon. Wea. Rev.,* **130**, 3008–3021, doi: 10.1175/1520-0493(2002)130<3008:EOEPOB>2.0.CO;2.

Watson, J. S., and S. J. Colucci, 1999: Is there a connection between Northern Hemisphere blocking and ENSO? Preprints, *Eighth Conf. on Climate Variations,* Denver, CO, Amer. Meteor. Soc., 30–33.

Wiedenmann, J.M., A.R. Lupo, I.I. Mokhov, and E.A. Tikhonova, 2002: The Climatology of Blocking Anticyclones for the Northern and Southern Hemispheres: Block Intensity as a Diagnostic. *J. Climate,* **15**, 3459–3473, doi: 10.1175/1520-0442(2002)015<3459:TCOBAF>2.0.CO;2.

Wilks, D. S., 1995: *Statistical Methods in the Atmospheric Sciences: An Introduction*. Academic Press, 467 pp.

University of Missouri Blocking Archive. Available online: http://weather.missouri.edu/gcc (accessed on 4 April 2017).